Studies on surface hoar : formation and physical properties
by Renee Maria Lang

A thesis submitted in partial fulfillment of the requirements for the degree of Master of Science in Engineering Mechanics
Montana State University
© Copyright by Renee Maria Lang (1985)

Abstract:
Field studies on surface hoar were conducted during the winter months of 1982-83 and 1983-84, at the Big Sky Ski Area, Big Sky, Montana. Mechanical shear strength tests, conducted on established surface hoar layers, indicated that although a layer would become visually undetectable, shear strength remained too low to measure for extended periods of time.

The initiation of surface hoar growth was dependent on a variety of near-surface and atmospheric conditions. Nocturnal clear-sky radiative heat loss from the snow surface did not necessarily predispose condensation onto the surface, although near-surface air temperature gradients would be in excess of +200°C/m.

A steady-state approximation for conservation of mass and momentum, in conjunction with the temperature data, predicts that surface crystal growth cannot be a diffusion limited process.

STUDIES ON SURFACE HOAR: FORMATION AND PHYSICAL PROPERTIES

by

Renee Maria Lang

A thesis submitted in partial fulfillment
of the requirements for the degree

of

Master of Science

in

Engineering Mechanics

MONTANA STATE UNIVERSITY
Bozeman, Montana

May 1985

Archives
N378
L255
cop.1

APPROVAL

of a thesis submitted by

Renee Maria Lang

This thesis has been read by each member of the thesis committee and has been found to be satisfactory regarding content, English usage, format, citation, bibliographic style, and consistency, and is ready for submission to the College of Graduate Studies.

May 15, 1985
Date

Theodore E. Langs
Chairperson, Graduate Committee

Approved for the Major Department

May 15, 1985
Date

Theodore E. Langs
Head, Major Department

Approved for the College of Graduate Studies

5-20-85
Date

Graduate Dean

STATEMENT OF PERMISSION TO USE

In presenting this thesis in partial fulfillment of the requirements for a master's degree at Montana State University, I agree that the Library shall make it available to borrowers under rules of the Library. Brief quotations from this thesis are allowable without special permission, provided that accurate acknowledgment of source is made.

Permission for extensive quotation from or reproduction of this thesis may be granted by my major professor, or in his absence, by the Dean of Libraries when, in the opinion of either, the proposed use of the material is for scholarly purposes. Any copying or use of the material in this thesis for financial gain shall not be allowed without my permission.

Signature 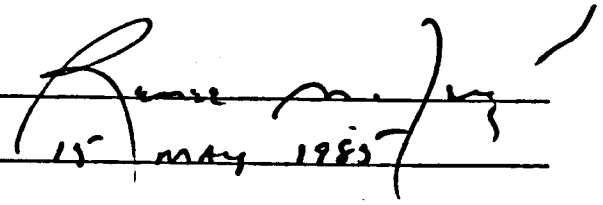

Date 15 May 1985

ACKNOWLEDGMENTS

I would like to express thanks to Brian R. Leo for his special photographic skills, and to Dr. Robert L. Brown for allowing me the freedom to investigate this topic.

The work reported here was done under National Science Foundation Grant No. CEE 7318476.

TABLE OF CONTENTS

		Page
APPROVAL		ii
STATEMENT OF PERMISSION TO USE		iii
ACKNOWLEDGMENTS		iv
TABLE OF CONTENTS		v
LIST OF FIGURES		vi
ABSTRACT		viii
Chapter		
ONE	INTRODUCTION	1
TWO	SITES AND INSTRUMENTATION	6
THREE	CASE STUDIES	11
	Study 1, 29-30 January 1984	11
	Study 2, 27-28 February 1984	16
	Study 3, 20 January–10 March 1983	23
FOUR	ANALYSIS OF THE CONDENSATION PROBLEM	29
FIVE	RESULTS AND CONCLUSIONS	41
LITERATURE CITED		45

LIST OF FIGURES

Figure		Page
1.	Crystal habit of ice grown in the atmosphere based on temperature and excess vapour density (Kobayashi, 1961)	4
2.	Group of surface hoar crystals exhibiting secondary growth features	5
3.	Thermocouple stack	7
4.	Use of shear frame	9
5.	Modified shear frame, underside view	10
6.	Temperature with respect to time at selected levels, 29-30 January 1984	13
7.	Accumulation of sector plates on the snow surface at approximately 1900 MST, 28-29 January	14
8.	Sector plates, 0300 MST, 28-29 January	15
9.	Time-averaged temperature profile for 2000–0300 MST, 29-30 January	17
10.	Curve-fit temperature profile	18
11.	Temperature with respect to time at selected levels, 27-28 February 1984	20
12.	Time-averaged temperature profile for 2000–0300 MST, 27-28 February	21
13.	Curve-fit temperature profile	22
14.	Upper portion of a single surface hoar crystal "in situ" on the snow surface at 1100 MST, 20 January 1983	24
15.	Same crystal as in Figure 14, after three hours of insolation	25
16.	In situ surface hoar layer, 43 days old	27
17.	Single surface hoar crystal, 50 days old	28

Figures

Page

18. $\delta(t)$ vs. t 32

19. Calculated near-surface thermal and concentration diffusion velocities for 29-30 January 38

20. Calculated near-surface thermal and concentration diffusion velocities, 27-28 February 39

ABSTRACT

Field studies on surface hoar were conducted during the winter months of 1982-83 and 1983-84, at the Big Sky Ski Area, Big Sky, Montana. Mechanical shear strength tests, conducted on established surface hoar layers, indicated that although a layer would become visually undetectable, shear strength remained too low to measure for extended periods of time.

The initiation of surface hoar growth was dependent on a variety of near-surface and atmospheric conditions. Nocturnal clear-sky radiative heat loss from the snow surface did not necessarily predispose condensation onto the surface, although near-surface air temperature gradients would be in excess of +200°C/m.

A steady-state approximation for conservation of mass and momentum, in conjunction with the temperature data, predicts that surface crystal growth cannot be a diffusion limited process.

CHAPTER ONE

INTRODUCTION

Surface hoar crystals are conventionally defined as plate-type ice crystals which form by deposition of water vapour onto the snow surface during the night. Due to their lack of intercrystalline bonding and weak attachment to the snow surface, accumulations of surface hoar form layers which are mechanically weak in shear. When such layers are buried by a subsequent snowfall, they provide excellent failure planes. The disaggregate crystals may act as lubricating layers, increasing the potential for slab avalanches. These same type of hoar crystals may also form a deposit on the surface of aircraft, changing the aerodynamic properties of the wings sufficiently to cause take-off problems (Henson and Longley, 1944).

To my knowledge, no previous thorough quantitative study of surface hoar growth has been conducted. Qualitatively, it has long been understood that surface hoar crystals normally develop during cold clear nights, when radiative cooling causes the snow surface temperature to fall below that of the contacting air. If the interfacial air becomes supersaturated with respect to the contacting ice surfaces, condensation occurs.

Subsequent snowfall on a surface hoar layer results in a mechanically unstable condition in the snowpack, conducive to slab avalanches. It has been suggested that "in many cases, surface hoar instability is relatively short-lived, lasting for only one or two storms" (Perla and Martinelli, 1976). This is a widely accepted hypothesis, yet relatively few clarifying measurements have been made.

The initiation of an avalanche is inevitably linked to shear failure within the snowpack. Hence, the shear strength of the various layers of snow within a seasonal snowpack

is a reliable indicator of slab avalanche stability/instability, and has been investigated by many authors (Haefeli, 1939; Roch, 1966; Keeler and Weeks, 1967; Martinelli, 1971; Voitkovsky, 1977; Perla, 1977; Perla, Beck, and Cheng, 1982). Attempts to correlate shear strength to parameters such as snow density, temperature and crystal size have produced erratic results (e.g., Perla et al., 1982). The most significant comparative measure of shear strength within a given layer of snow seems to be the degree of intercrystalline bonding, which is directly related to crystal morphology.

Although all ice crystals which occur at atmospheric temperatures and pressure possess the same basic hexagonal crystalline structure (the hexad symmetry axis is the c-axis, and perpendicular to it are the three a-axes at 60° to each other), they exhibit a large variety of shapes. The more spherical forms of ice crystals are sometimes referred to as equilibrium growth forms, since they are known to develop under isothermal or near-isothermal conditions (Colbeck, 1982). These spherical grains are usually associated with a high degree of intercrystalline bonding. Within the snowpack, they develop at the expense of the more faceted forms. Layers of these grains or clusters will remain mechanically stable unless free water is present within the snowpack. Faceted forms of ice crystals, or the kinetic growth forms, can be completely cohesionless. This is especially true in the case of plate-type (i.e., preferential growth along the a-axes) ice crystals such as surface hoar. Furthermore, when the nucleation site of a surface hoar crystal is a pre-existing snow crystal, it is also ineffectively bonded at that point. Hence, once incorporated into the snowpack, a layer of surface hoar crystals form a shear failure plane. The layer remains weak until the individual crystals metamorphose into a more mechanically stable form. This, of course, cannot occur unless the kinetic growth form becomes thermodynamically unstable with respect to its environment.

The basic crystal habit of kinetic growth forms is governed by temperature (Nakaya, 1954; Shaw and Mason, 1955; Kobayashi, 1957, 1961; Hallett and Mason, 1958). Observed

changes in habit are not a consequence of changes in the diffusion field but are dependent on some temperature sensitive property of the crystal surface (Mason et al., 1963). Under laboratory conditions, preferential a-axis growth was found to occur within two sharply defined temperature regimes (Fig. 1), 0°C to -4°C, and -10°C to -22°C (Kobayashi, 1961). The secondary growth features, such as the "feathery" or "dendritic" extensions of plates, commonly associated with surface hoar (Fig. 2), are a consequence of degree of excess vapour density. Hence, surface hoar growth should occur only at temperatures where the crystal may begin as a thin plate and at some degree of supersaturation (Mason et al., 1963).

However, the growth of ice crystals under various laboratory conditions cannot be expected to describe the condensation process at a snow surface of ever-changing temperature exposed to the atmosphere. The purpose of this investigation was to more fully understand the formation, physical properties and subsequent metamorphism of surface hoar. To accomplish this, a detailed field study has been carried out. Shear strength tests were conducted on established surface hoar layers and observations were made in order to determine the conditions under which the layer would metamorphose to a more stable equilibrium form. A correlation of progressive surface hoar development on a snow surface, with near-surface snow and air temperatures, snow surface temperature, initial snow surface conditions, horizontal air motion, and general atmospheric conditions was determined. The temperature and condensation rate data were used concomitantly with expressions for conservation of mass and momentum, and diffusive vapour flux in order to estimate some of the broader aspects of mass transport phenomena at a snow surface.

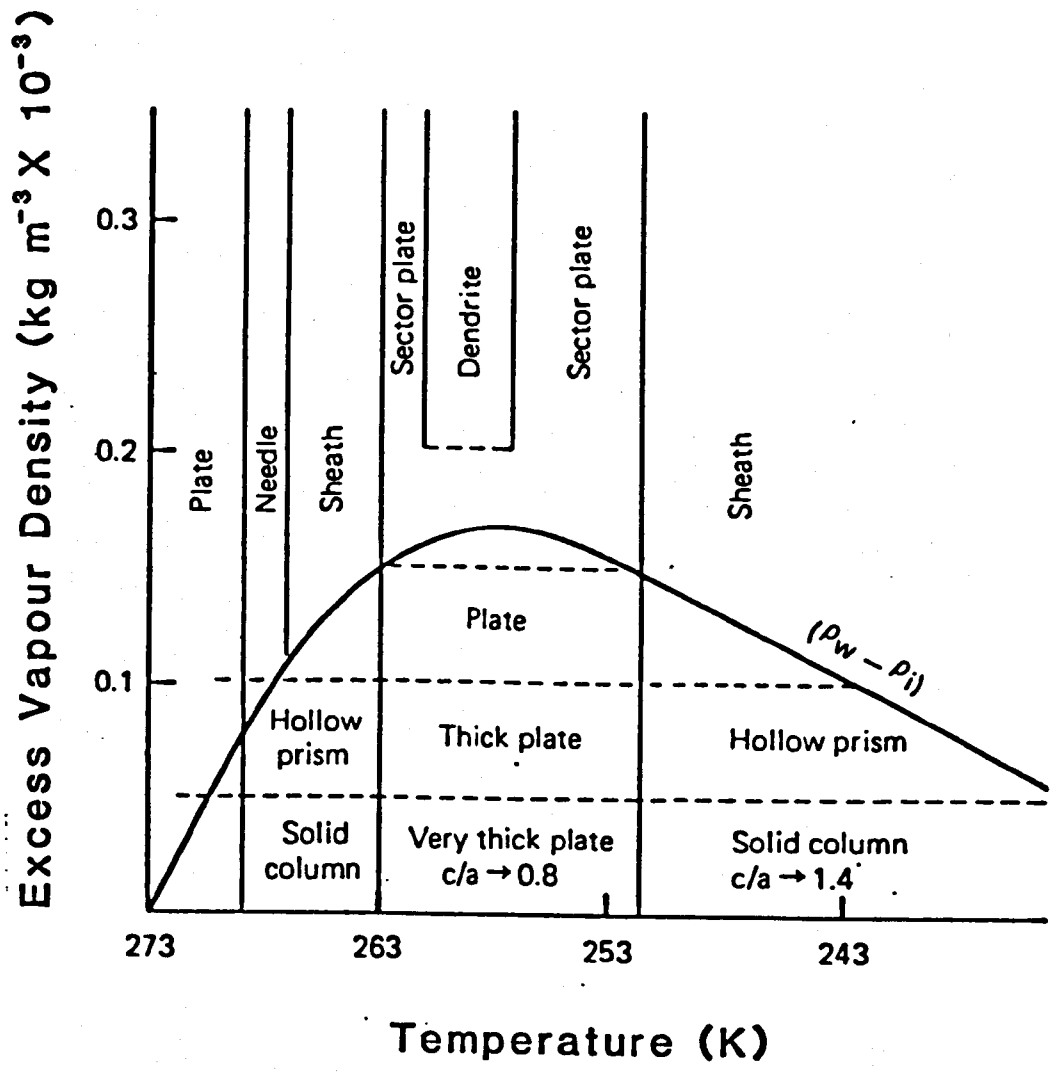

Figure 1. Crystal habit of ice grown in the atmosphere based on temperature and excess vapour density (Kobayashi, 1961).

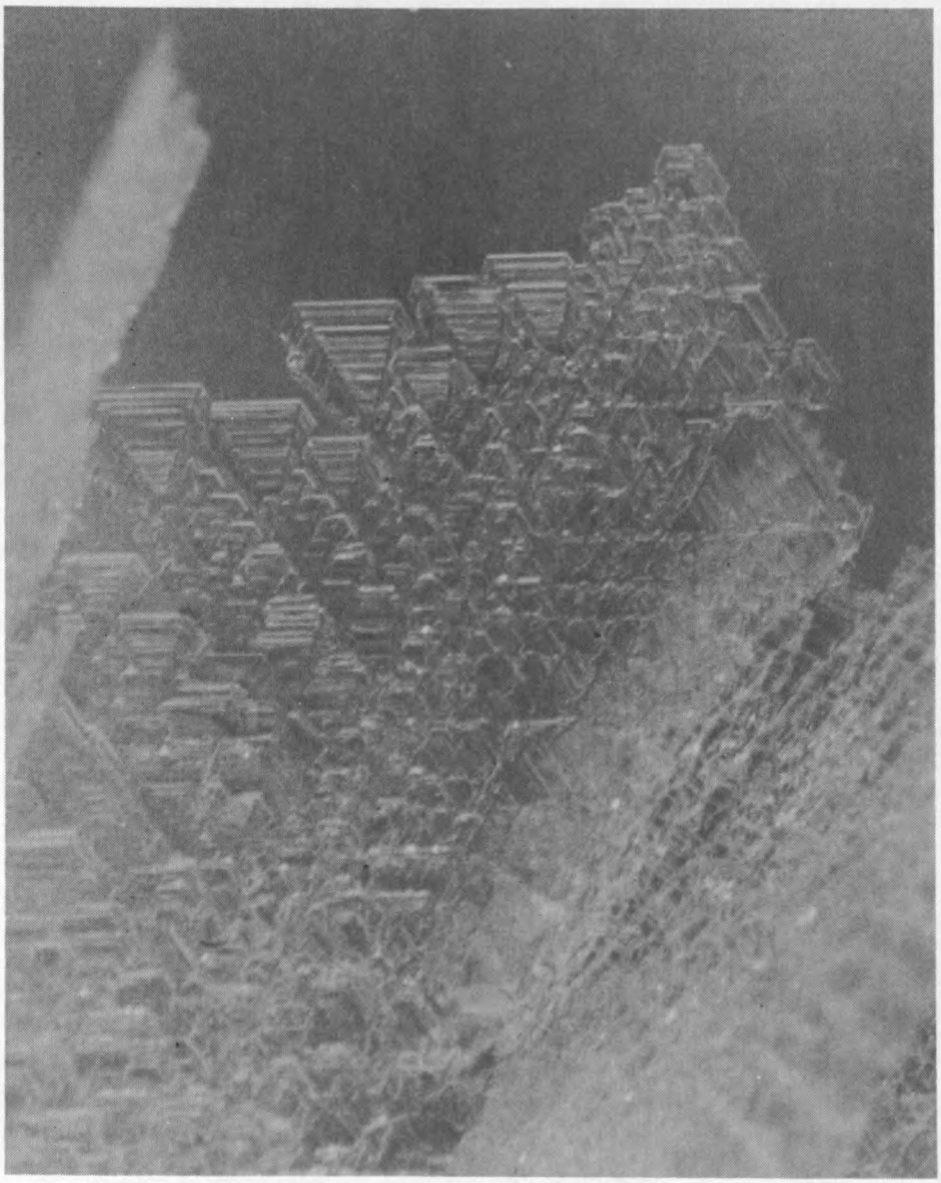

Figure 2. Group of surface hoar crystals exhibiting secondary growth features.

CHAPTER TWO

SITES AND INSTRUMENTATION

Night-time observations of surface crystal growth were made at a large, topographically flat area (elevation 2680 m) located within the Big Sky Ski Area, Big Sky, Montana. The area is relatively free from any obstacles which could cause significant back-radiation to the snow surface. Measurements were made on numerous occasions during the winter months of 1982-83 and 1983-84, and in only a few cases did actual surface hoar development occur.

Profiles of temperature were obtained hourly by using two separate stacks of copper-constantan thermocouples (Fig. 3). Temperatures were obtained at .5, 1.0, 1.5, 2.0, 3.0, and 4.0 cm above the snow surface, at the surface, and at depths of 1.0 and 2.0 cm in the snow. During each experiment, one thermocouple was shielded with an aluminum cone in order to determine radiational effects on temperature measurements. No significant changes were detected at any level with this method.

Any significant near-surface horizontal air movement was detected by placing "flags" of net-type material at various levels.

Time-lapse photography was used, with limited success, in order to obtain an estimate of the condensation rate.

General weather patterns were also recorded.

Shear strength measurements on established surface hoar layers were conducted on an undisturbed north-facing slope located within the Big Sky Ski Area, Big Sky, Montana. Due to the fragile nature of surface hoar, it must be tested "in situ." Devices developed previously for testing the shear strength of alpine snow have not displayed consistent

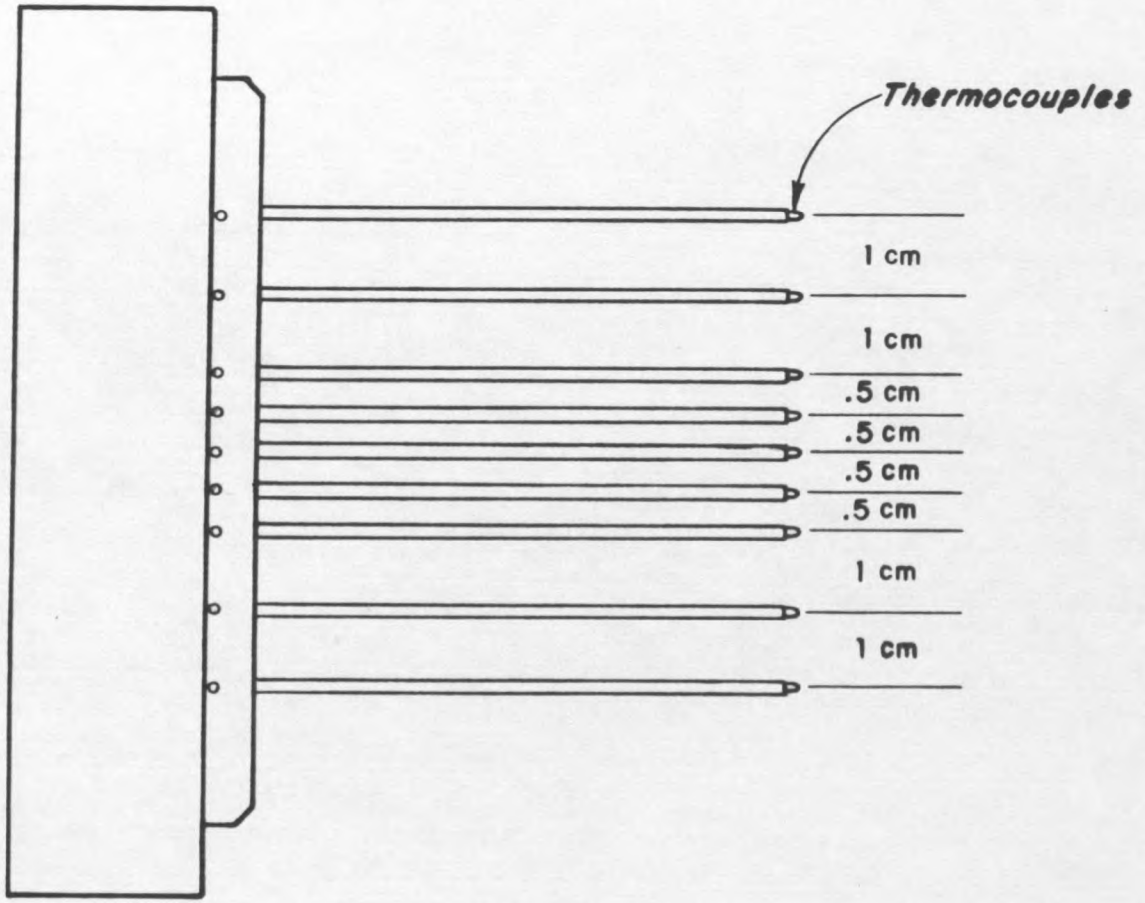

Figure 3. Thermocouple stack.

results. Furthermore, they are not sensitive enough to give a measurable value of shear strength for such low strength layers such as surface hoar. These mechanisms were therefore considered unsuitable. A modification of the device commonly referred to as the standard shear "frame" (Roch, 1966) was used instead. This revised shear "frame" (Brown and Oakberg, 1982) provides a more equally distributed force throughout the snow sample by introducing a series of small protrusions, each of which absorbs a small portion of the compressive force exerted on the snow sample during testing (Figs. 4 and 5). The "pull" device and gauge are located at the base of the frame such that angular deviations from a direction parallel to the layer do not occur, thereby reducing "user dependence" and giving a more consistently accurate measure of actual shear strength.

The area of the modified frame is .0001 m^2. The maximum variation on a given layer at a certain stage, when performing ten tests as suggested by Perla (1977), was less than 200 Pa. A slow "rate of pull" was used and tests were not limited to one "user."

Shear strength measurements and a photographic record of the deterioration of the hoar were made on a weekly basis.

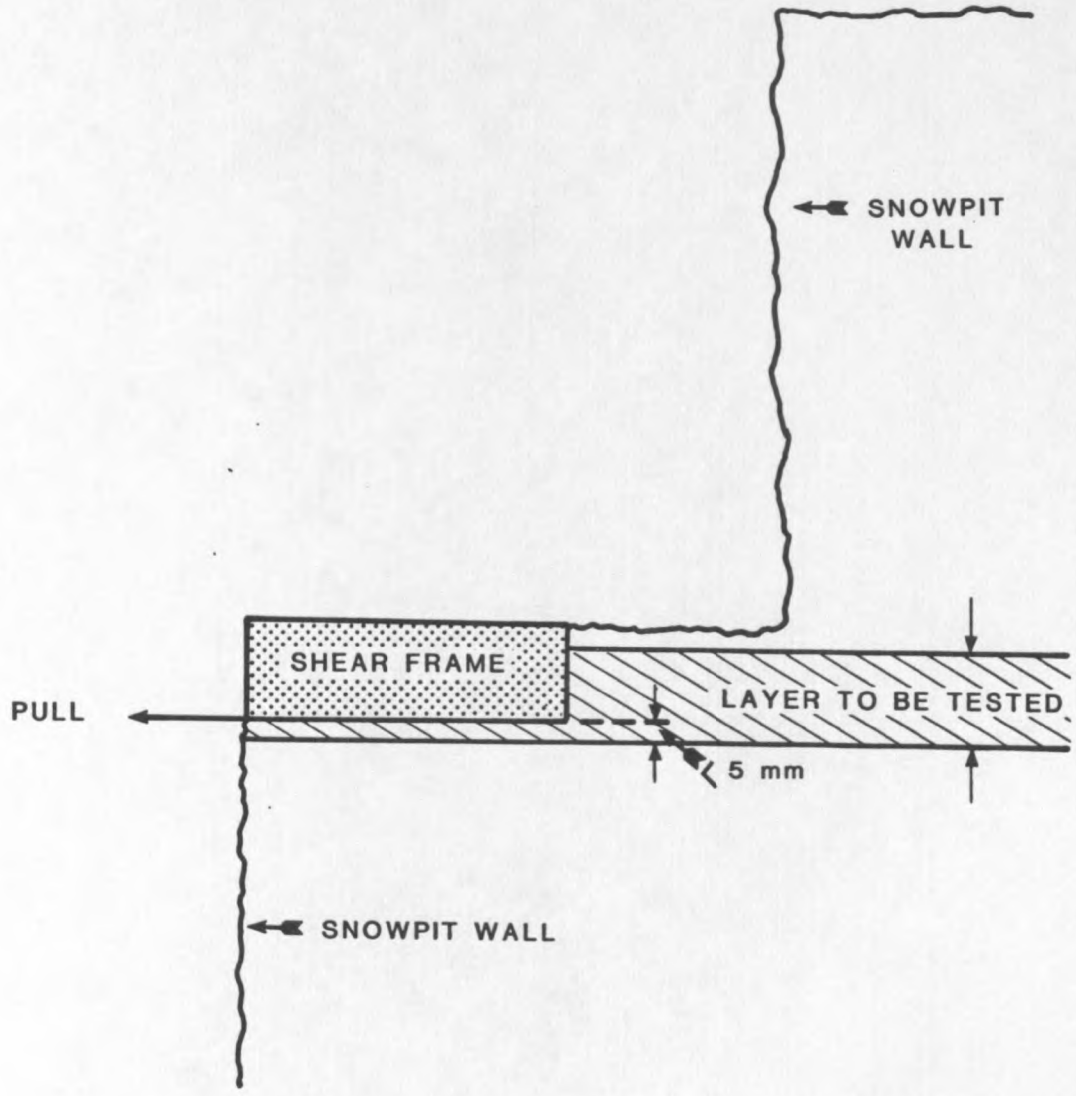

Figure 4. Use of shear frame.

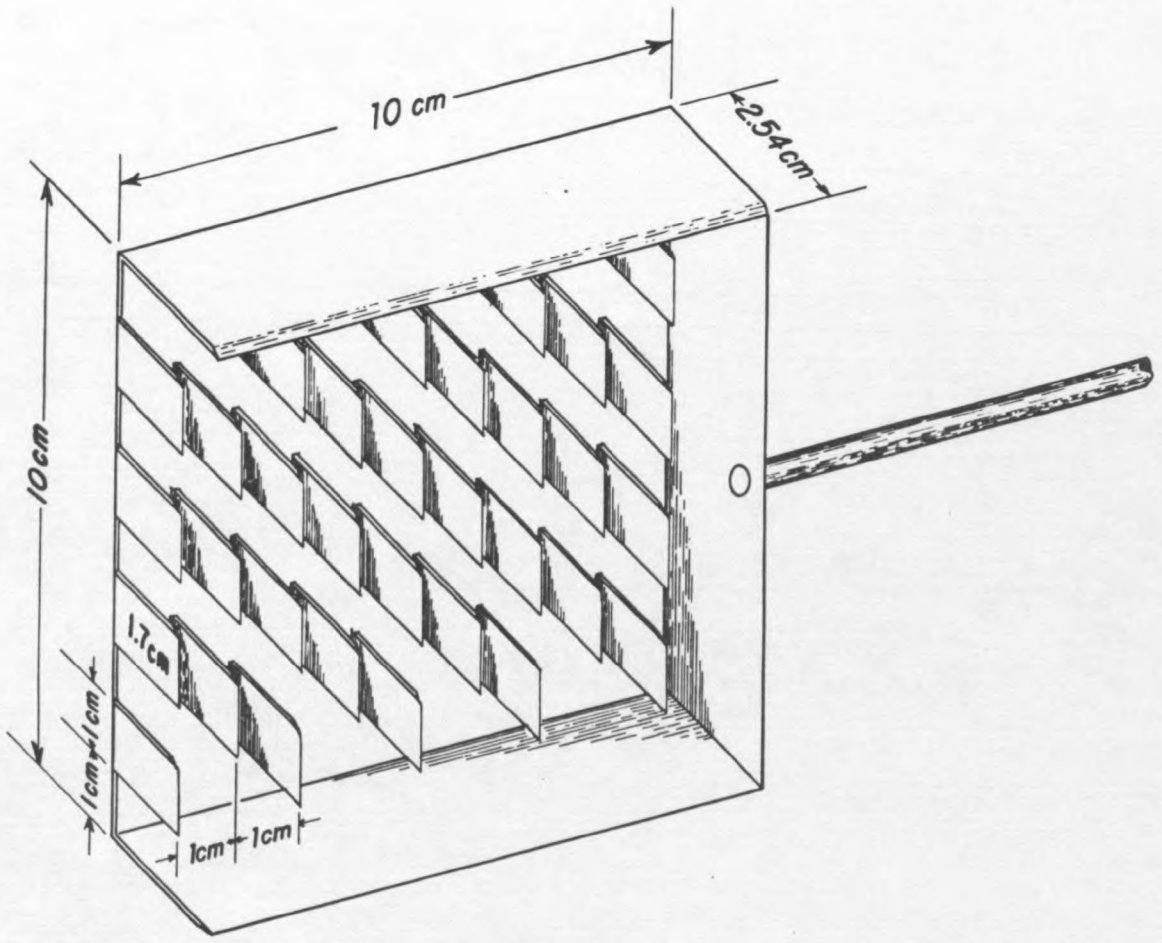

Figure 5. Modified shear frame, underside view.

CHAPTER THREE

CASE STUDIES

The results of three representative field studies are described. The first and second are nighttime growth studies in which surface hoar was deposited to an average height of 1.3 to 1.5 cm. It should be mentioned that in over 60% of observed cases, surface crystal growth did not occur under nocturnal clear-sky conditions. In many cases, needle-type growth (i.e., preferential growth along the c-axis) occurred, but shortly after sunrise the needles would be sublimated away. This may serve to explain why surface hoar is always described as plates (see for example, LaChapelle, 1969), while the term depth hoar is used to describe any kinetic growth form which develops within the snowpack. In all cases, measured temperature profiles were similar unless a strong breeze persisted or cirruform interferred. Time-averaged temperature profiles over the period of estimated maximum condensation were curve-fit by use of the Simplex method (Nedler and Mead, 1965; Caceci and Cacheris, 1984), adapted to run under the VAX/VMS operating system.

The third case study describes a series of shear strength tests and a photographic record of an established surface hoar layer.

Study 1, 29-30 January 1984

1500 MST – The snow surface was composed of freshly fallen, stellar and rimed-stellar snow. A heavy cumulus cloud cover, accompanying the passage of a cold front had lingered all day.

1800 MST – Only a few cirrus and altocumulus lenticularis cloud forms remained. The air between 1.0 and 4.0 cm above the surface was nearly isothermal at approximately

-13.0°C, although a gradient in excess of +200°C/m had already been established between the snow surface (-14.8°C) and air .5 cm above the surface (-13.4°C). A negative temperature gradient had been established in the snow adjacent to the surface; the snow temperature at 2.0 cm below the surface was approximately -14.1°C (see Fig. 6 for temperature transitions at selected levels with respect to time).

1900 MST – Skies were perfectly clear. The snow surface had cooled to -16.6°C. The adjacent snow and air were cooling at slightly lower rates. No hoar growth was noticeable, but macro-photography revealed that sector plates had begun to accumulate (Fig. 7).

2000 MST – Skies remained clear. The snow surface reached its minimum temperature of -18.7°C. The air-snow surface temperature gradient was nearly linear at approximately +140°C/m. Similarly, the snow-snow surface temperature gradient was nearly linear at approximately -80°C/m. Sector plates had accumulated to an average height of .25 cm.

2300 MST – Skies remained clear. The snow at the measured depth 1.0 cm had become nearly isothermal with respect to the snow surface. The maximum temperature difference between the snow surface (-18.5°C) and the air at +4.0 cm (-12.8°C) had been reached. The hoar crystals were approximately .5-.7 cm high.

0000 MST – Skies remained clear. The maximum positive temperature gradient (+380°C/m) between the original snow surface (-16.4°C) and the adjacent air at +.5 cm (-14.5°C) was attained. (Note: in most other case studies when condensation occurred the gradient at this time would be in excess of +300°C/m.) A positive gradient (+70°C/m) had been established between the snow at -2.0 cm (-17.8°C) and the snow surface (-16.4°C). (This phenomenon of temperature gradient reversal was also consistently observed to occur.)

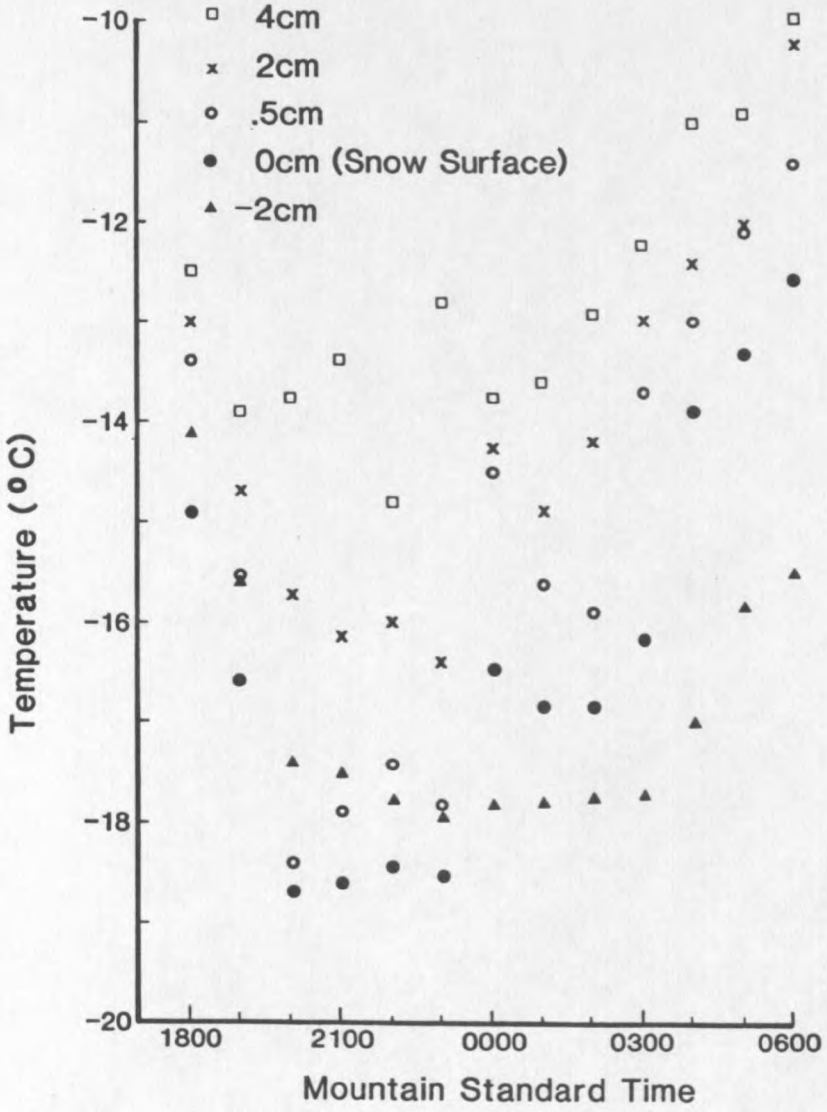

Figure 6. Temperature with respect to time at selected levels, 29-30 January 1984.

Figure 7. Accumulation of sector plates on the snow surface at approximately 1900 MST, 28-29 January. Wire diameter is < .5 mm.

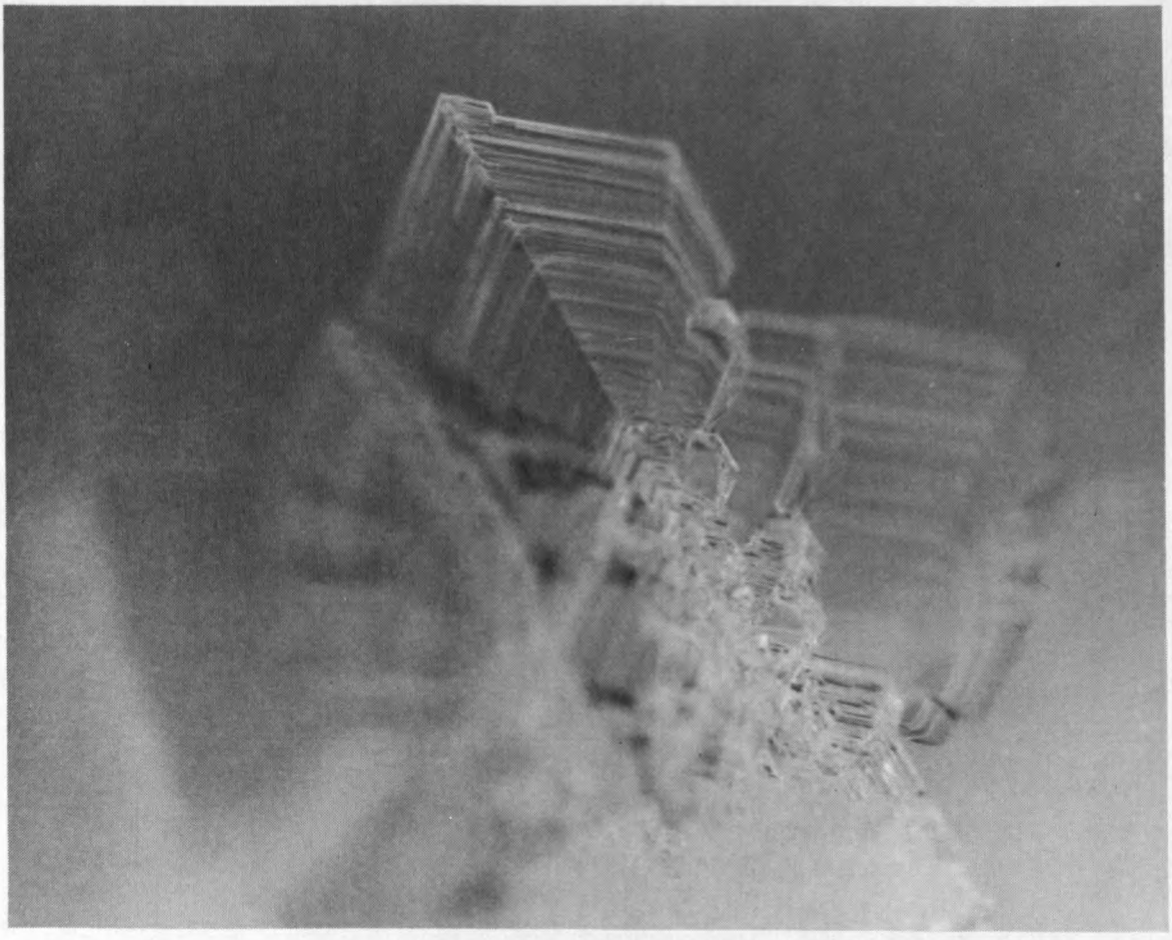

Figure 8. Sector plates, 0300 MST, 28-29 January.

0300 MST – Skies remained clear. The hoar plates reached their maximum size of 1.3-1.5 cm in height (Fig. 8). No secondary growth features were observed.

0600 MST – The experiment was terminated. No horizontal air motion within 1.0 m of the snow surface had been detected all night. A positive temperature gradient in both the snow and air persisted until this time. Skies had remained clear all night.

A time-average of the overall temperatures during the maximum growth period (2000-0300 MST) is represented in Figure 9. Note that the overall effect of the temperature gradient reversal in the upper 2.0 cm of the snow is a near isothermal time-average. A curve-fit of the time-averaged temperature is represented in Figure 10.

Study 2, 27-28 February 1984

1500 MST – The snow surface was composed of stellar snow resulting from a storm which had occurred on 25-26 February. Cirrus cloud forms were present and a slight breeze persisted. Due to the frontal passage and the initial snow surface temperature (-9.7°C) hoar growth was expected. Two additional tests were conducted. A black plastic sheet 1 m^2 was placed onto a section of the snow surface, the plastic being intended to form a vapour barrier between the snow and the atmosphere. Hence if the vapour flux from the snow to the snow surface was significant in supplying vapour for condensation, then the amount of condensate onto the plastic should be minimal. Also, a stainless steel substrate 20 cm^2 was placed above the snow surface in order to determine how effectively the condensate would bond to the metal surface. Of course, due to the diverse properties of the various surfaces, the net accumulation of hoar was expected to be quite variable.

1800 MST – The breeze was persisting, but the skies had cleared. A temperature gradient of approximately +380°C/m had been established between the snow surface (-15.8°C) and the air at .5 cm above the surface (-13.9°C). A negative temperature

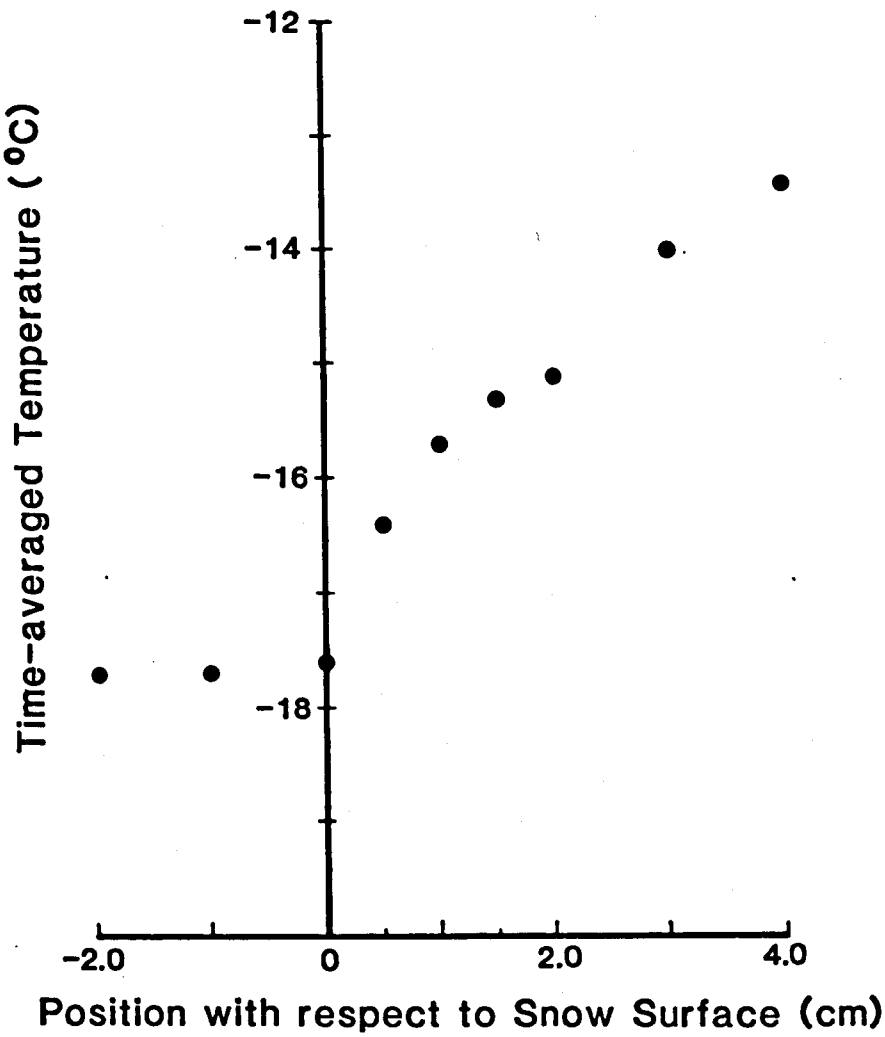

Figure 9. Time-averaged temperature profile for 2000–0300 MST, 29-30 January. Zero position is original snow surface.

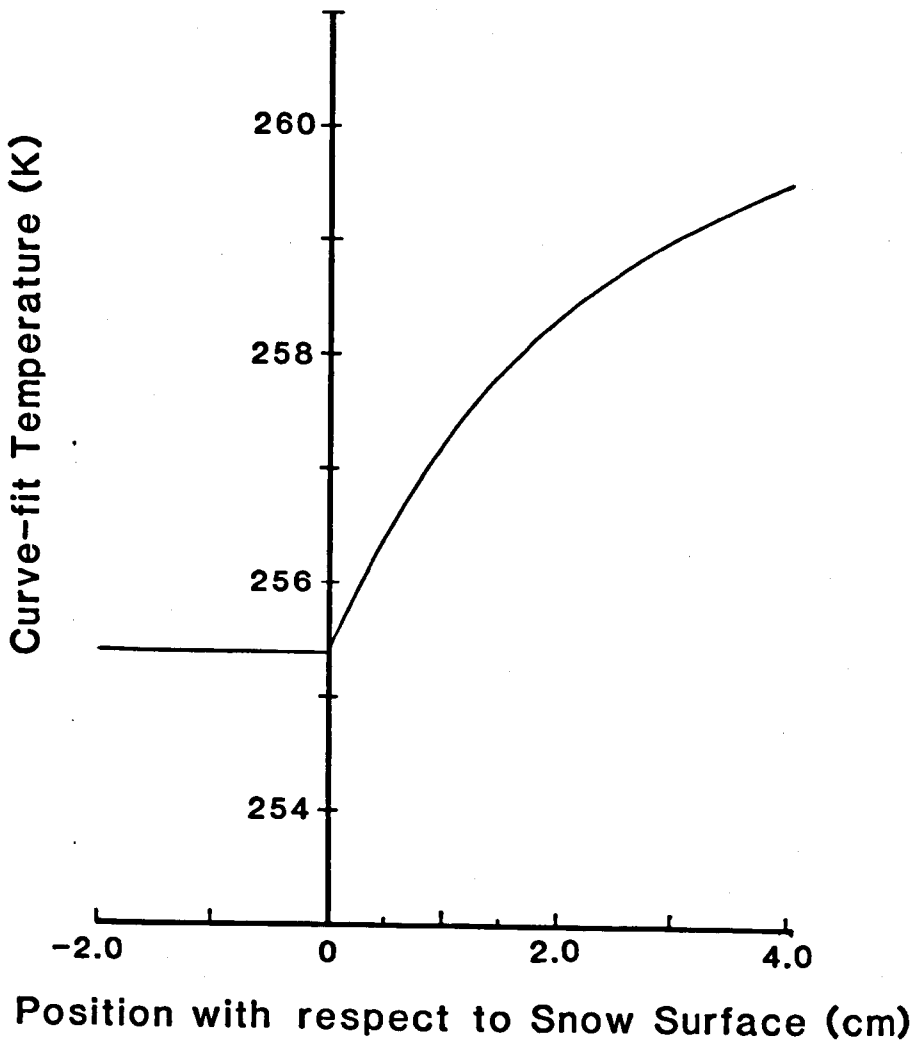

Figure 10. Curve-fit temperature profile. For $z \geq 0$, $\Theta \doteq (6.86z/(2.64 + z)) + 255.55$.

gradient (approximately -99°C/m) had been established in the snow adjacent to the surface.

1900 MST — No breeze was detectable. The snow surface had continued to cool to approximately -18.7°C. The air had cooled very rapidly at the levels less than 2.0 cm, such that the temperature gradient in the air was approximately linear at +161°C/m. Similarly, a nearly linear negative gradient in the adjacent snow existed (approximately -108°C/m). (See Fig. 11 for temperature transitions w.r.t. time.) Skies were clear.

2100 MST — Sector plates had accumulated to an approximate average height of 0.5 cm on all surfaces. Skies remained clear and at this time a very large temperature difference existed between the original snow surface (-19.6°C) and the air at 0.5 cm (-16.5°C).

2200 MST — The air and snow at all levels reached their minimum temperatures. The snow surface temperature was at -20.5°C. Skies were clear.

0100 MST — The temperature gradient in the snow had reversed in the upper 1.0 cm to +5°C/m. The plates were approximately 1.0-1.2 cm in height on all surfaces. Skies remained clear.

0300 MST — The hoar plates reached their maximum average height of 1.2-1.5 cm. No secondary growth features were observed.

0600 MST — The experiment was terminated. Skies had remained clear throughout the night. No horizontal air motion was detected after 1900 MST. The plates were approximately the same size on all surfaces. The plates which had condensed onto the stainless steel substrate were more uniformly oriented in a surface normal direction, and were indeed firmly attached at their nucleation site.

The time-averaged temperature profile and curve-fit profile during the period of maximum observed condensation are presented in Figures 12 and 13, respectively. In

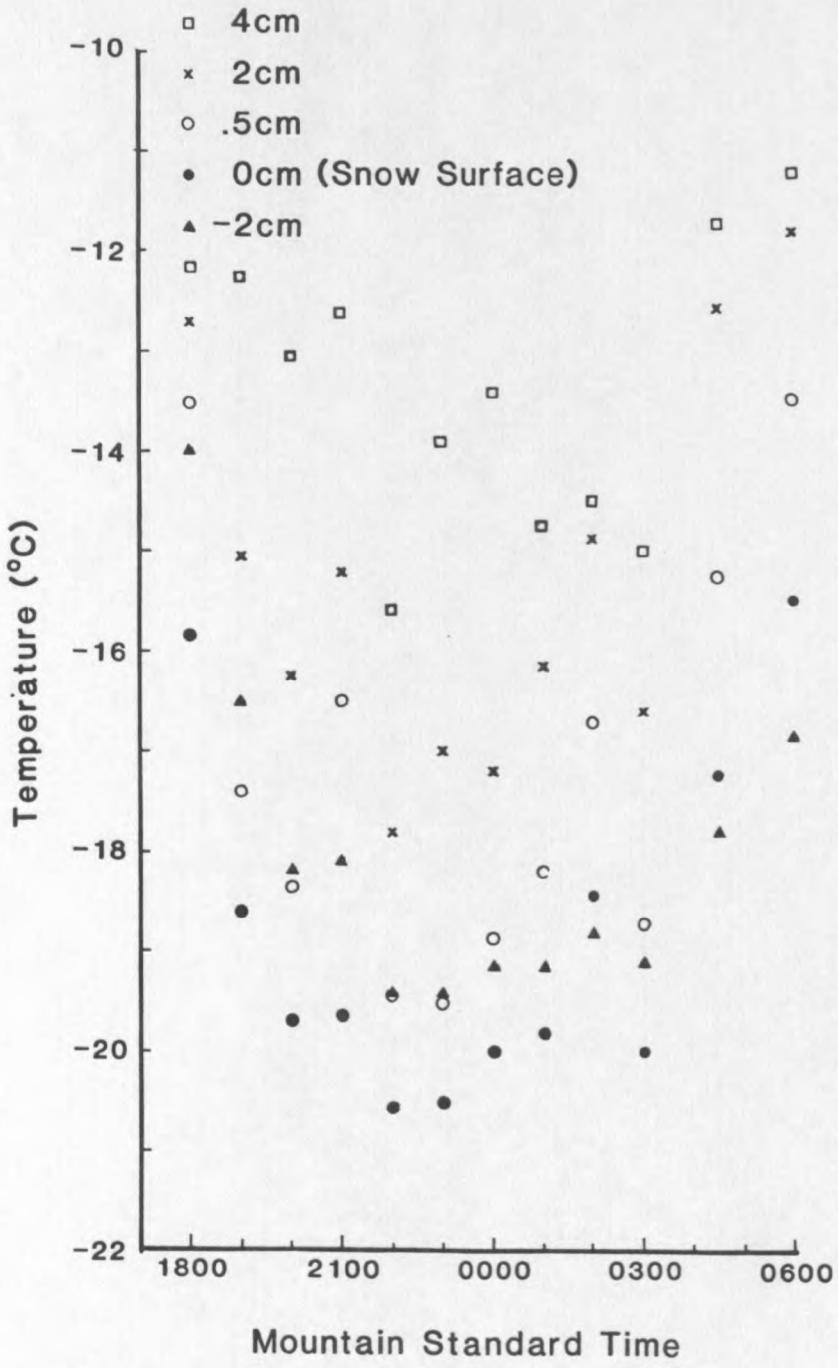

Figure 11. Temperature with respect to time at selected levels, 27-28 February 1984.

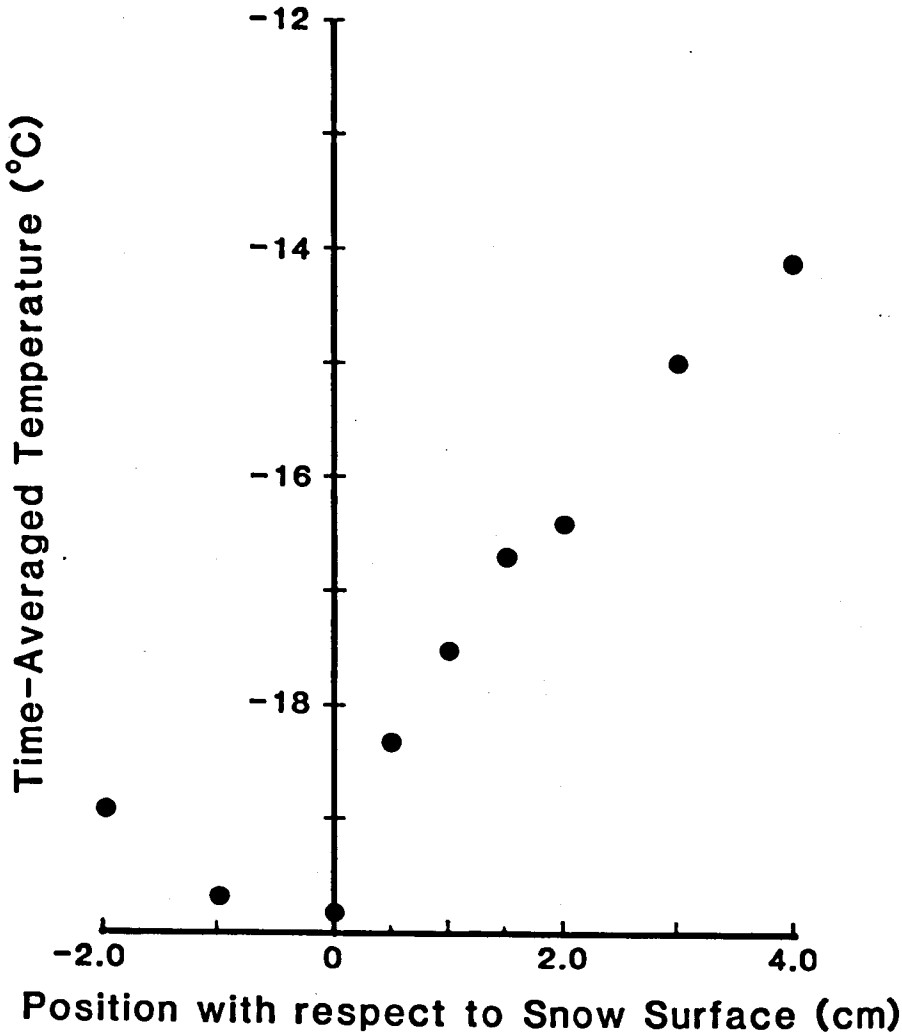

Figure 12. Time-averaged temperature profile for 2000-0300 MST, 27-28 February.

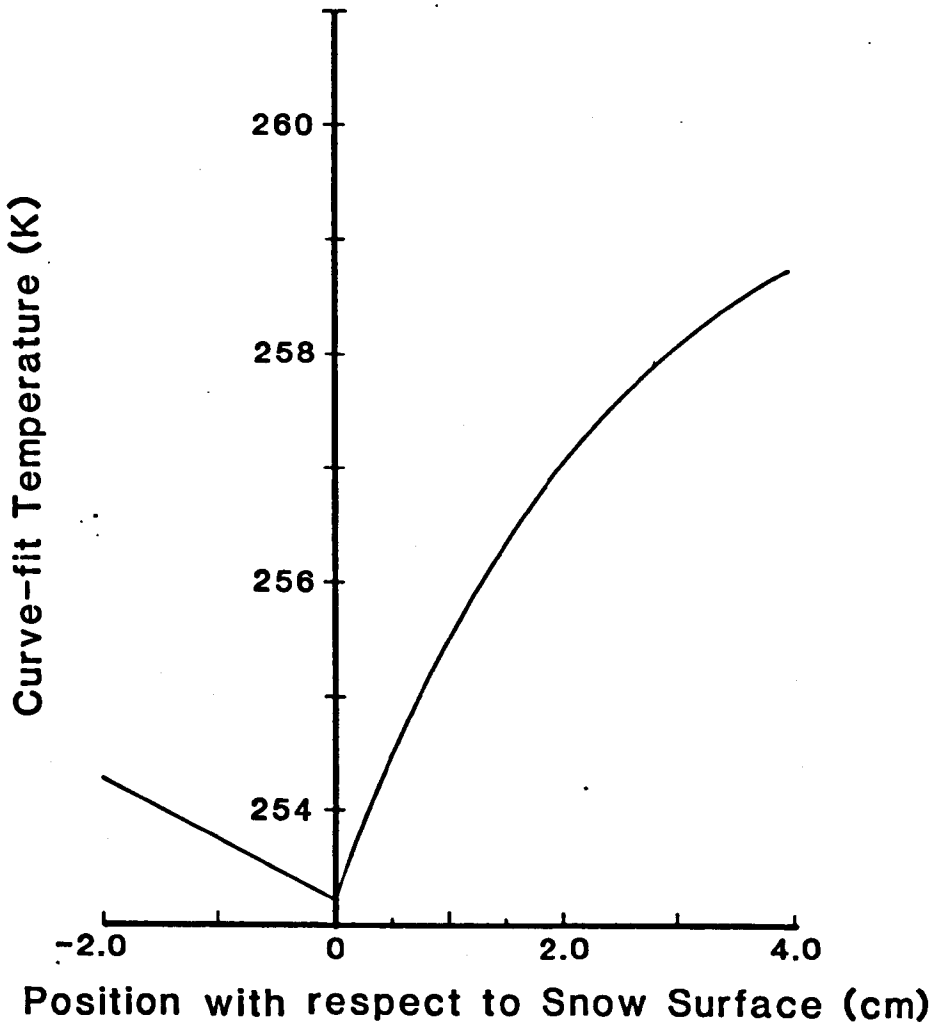

Figure 13. Curve-fit temperature profile. For $z > 0$, $\Theta \doteq (10.77\ z/(3.66 + z)) + 253.35$.

this particular case, a net negative temperature gradient had persisted in the upper 2.0 cm of the snowpack.

Study 3, 20 January–10 March 1983

20 January – Extremely well-developed surface hoar, averaging 4.0–5.0 cm in height, had been deposited onto the snow surface during two previous nights (18-19 and 19-20 January). Time lapse photography of a single crystal in situ, between 1100 and 1400 MST, during which time clear-sky conditions persisted, was conducted in order to determine the effects of insolation on the crystal. The photographs revealed that the typical "feathery" or dendritic secondary growth features of the hoar are an aggregation of separately developing sector plates oriented either on or at 60° to the predominant a-axis (Fig. 14), as reported by Mason et al. (1963). Three hours of insolation served to reduce the individual peripheral plates by insignificant amounts in comparison to the total size of entire crystal (Fig. 15). A temperature gradient, in excess of +200°C/m, between the base and top of the crystal, persisted throughout this time.

27 January – The layer was covered by 10 cm of low density snow. Structural changes of the surface hoar were minimal. It was very well adhered to the adjacent snow above, but shear strength at the base of the layer was too low to measure (i.e., less than 25 Pa).

3 February – The peripheral edges of the crystals had rounded and pore spaces had become loosely filled with granular snow. Basal shear strength had increased to an average of 35 Pa.

11 February – The layer was buried under 46 cm of low density snow, but was still recognizable, although individual crustals had deteriorated into a more "axial" form. The average basal shear strength had slightly decreased to an unmeasurable average.

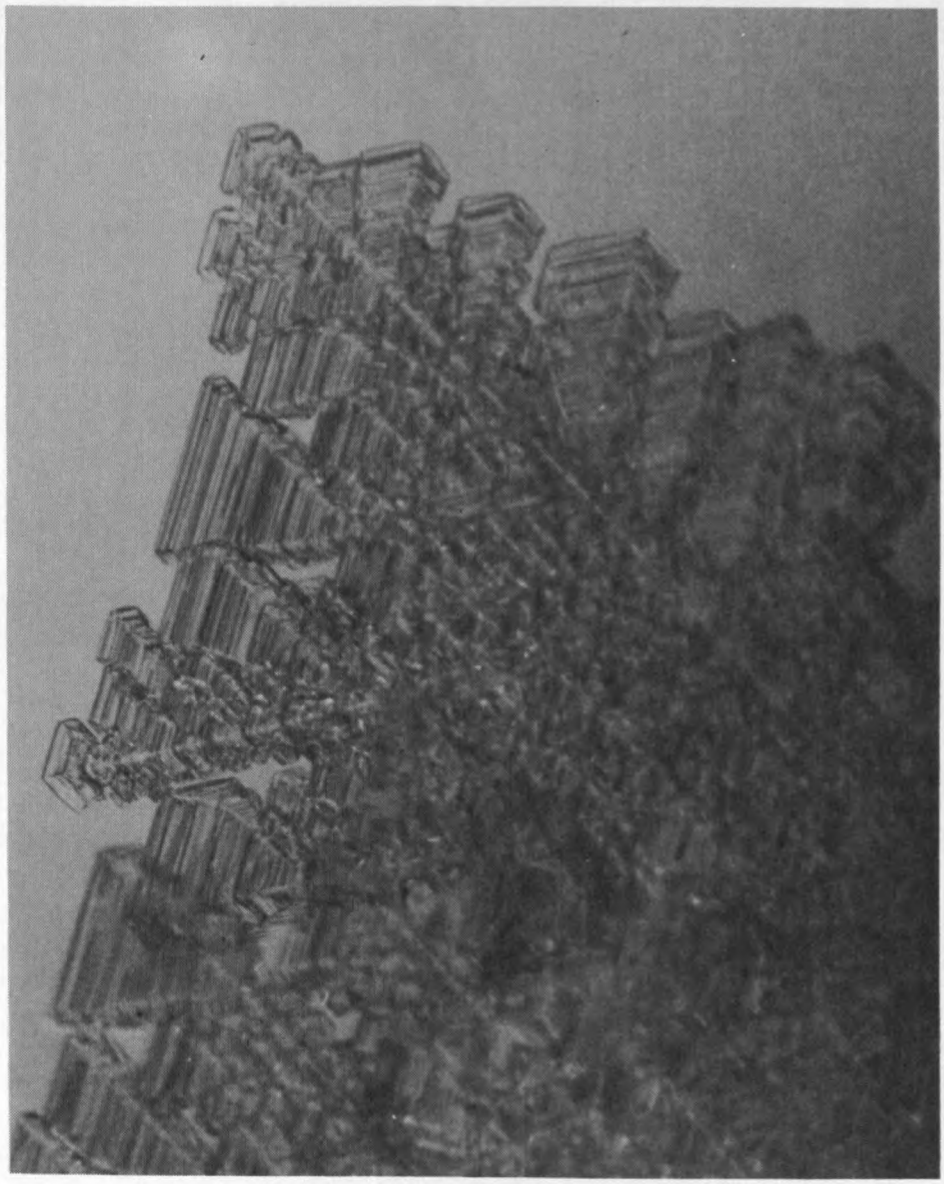

Figure 14. Upper portion of a single surface hoar crystal "in situ" on the snow surface at 1100 MST, 20 January 1983.

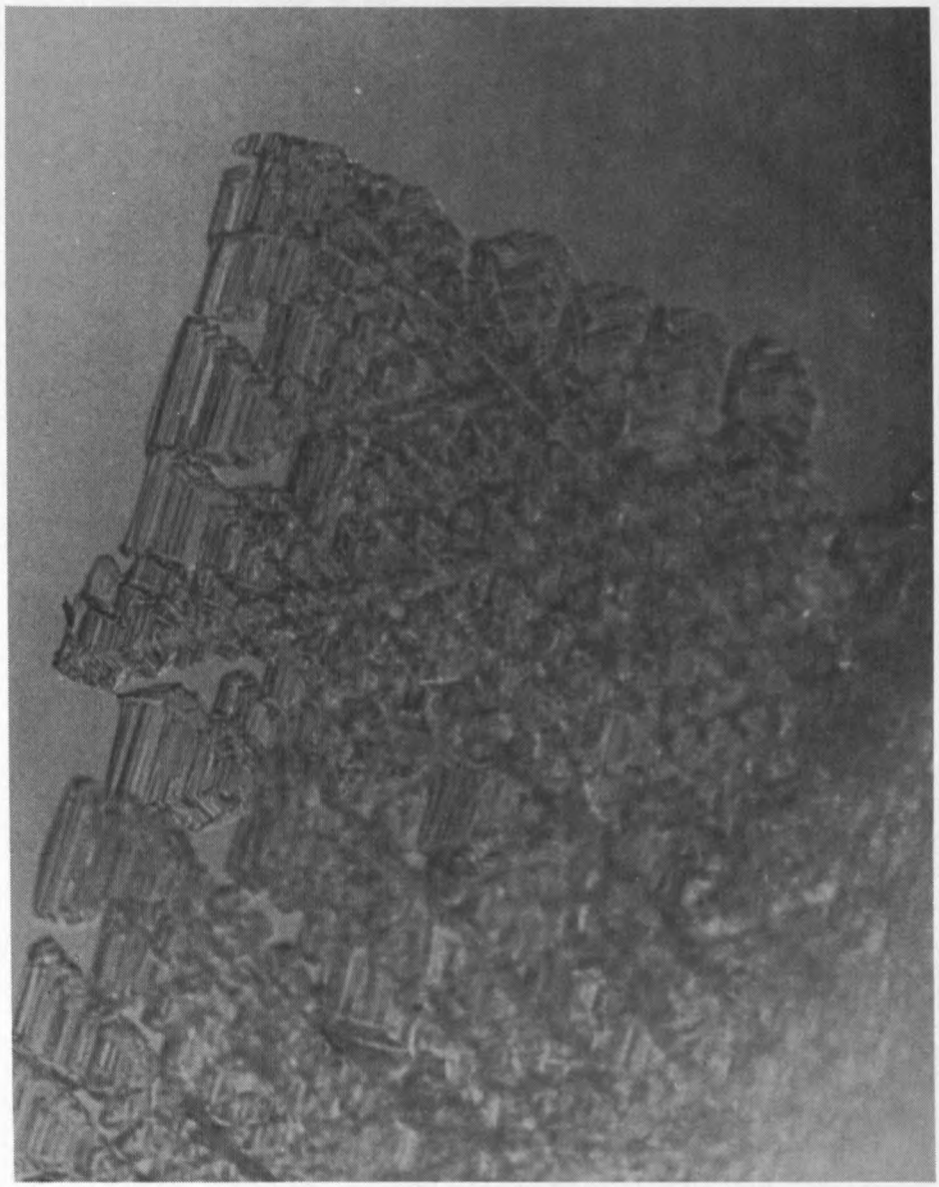

Figure 15. Same crystal as in Figure 14, after three hours of insolation.

4 March – The layer had become nearly "hollow" (Fig. 16), i.e., the crystals had deteriorated such that only the largest remained visible. The snow below was now composed entirely of well-rounded grains. Basal shear strength had increased to approximately 110 Pa.

10 March – It was very difficult to detect the layer, yet the crystals were still quite large (Fig. 17). The layer was obscured due to the degree of rounding of the hoar edges and bonding of the hoar to well-rounded grains which had completely filled the pore spaces. Average basal shear strength was 390 Pa.

After this date, free water in the snowpack destroyed the layer.

Figure 16. In situ surface hoar layer, 43 days old.

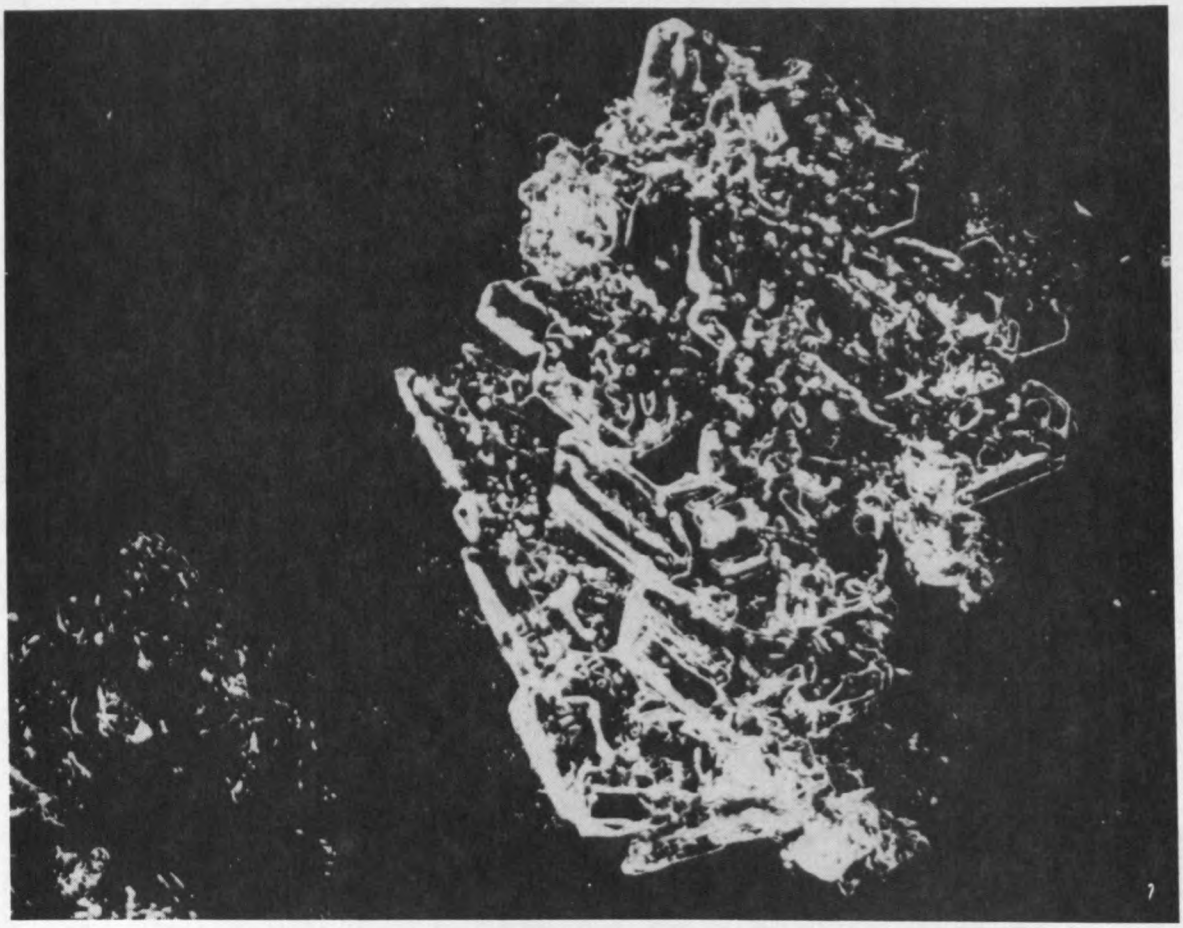

Figure 17. Single surface hoar crystal, 50 days old.

CHAPTER FOUR

ANALYSIS OF THE CONDENSATION PROBLEM

Due to the complexity of even the simplest of atmospheric flows, some preliminary assumptions must be made. As a first approximation, it will be assumed that motion occurs only in the surface-normal direction, taken to be the z-coordinate direction.

One main difficulty is the definition of some precise physical boundary, i.e., the exact position of the "snow surface" at some time t. In order to make the problem determinate, it will be assumed that the initial snow surface is located at $z=0$ at some time $t=0$, prior to condensation. At some time $t>0$, the snow/atmosphere interface is located at $\delta(t)>0$, i.e., the growth rate of each single ice crystal is assumed to be uniform. Hence, the interface is defined as the small region where the phase change from vapour to ice (or vice versa) is occurring.

The mass flux to/from the underlying snow at $z<0$ is assumed to be negligible. Motion in the x and y directions is neglected.

Transport properties were extrapolated from experimentally obtained values (Mason and Monchick, 1963). Saturation state values were extrapolated from Keenan and Keyes (1978).

The temperature profile above $z=0$ was taken to be constant with time at the onset of condensation, and values were obtained from the curve-fit profiles (shown in Figs. 10 and 13).

In any non-isothermal multicomponent mixture of $\alpha=1,2,\ldots n$ constituents, mass must be conserved for each constituent and also for the mixture. Hence $n+1$ equations may be written for conservation of mass, of which only n are independent.

Assuming that any vapour being removed at the snow surface is being replaced from above, conservation of mass for steady, one-dimensional flow of vapour may be written as

$$\frac{d}{dz}(\rho_v \dot{z}_v) = \hat{m}_v, \tag{1}$$

where ρ_v is the local or dispersed density of the vapour, $\dot{z}_v$ is the velocity of the vapour, and $\hat{m}_v$ is defined as the mass "exchange" or "production" (see for example Luikov and Mikhailov, 1965) for the vapour, and represents a transfer from vapour phase matter to solid phase, or vice versa.

Since the ice essentially retains no velocity, conservation of mass for the ice phase matter may be expressed as

$$\frac{d\rho_s}{dt} = \hat{m}_s \tag{2}$$

where ρ_s represents the dispersed density of the ice and may also be expressed as

$$\rho_s = \gamma_i \nu_i \tag{3}$$

where γ_i is the mass density of the ice grain itself and ν_i is the volume distribution function of the solid phase matter.

Conservation of mass for the air is

$$\frac{d}{dz}(\rho_a \dot{z}_a) = 0, \tag{4}$$

then for the entire mixture

$$\frac{d\rho_s}{dt} + \frac{d}{dz}(\rho_v \dot{z}_v + \rho_a \dot{z}_a) = \hat{m}_s + \hat{m}_v. \tag{5}$$

Obviously, this requires

$$\hat{m}_s + \hat{m}_v = 0, \tag{6}$$

which in turn gives the following relationship;

$$\frac{d}{dz}(\rho_v \dot{z}_v) = \frac{-d\rho_s}{dt} \tag{7}$$

Then, assuming that the time rate of change of the dispersed ice density is constant for steady state conditions,

$$\rho_v \dot{z}_v = C_1 z + C_2 \tag{8}$$

$$-\rho_s = C_1 t + C_3 \tag{9}$$

where C_1, C_2, C_3 are constants. Define $\dot{m}$ as the condensation rate, σ as the condensation coefficient or the fraction of the vapour flux impinging on the snow surface which actually condenses, and $d\delta/dt$ as the time rate of change of the position of the interface. Then

$$-\sigma\rho_v \dot{z}_v = \dot{m}, \qquad z=\delta \tag{10}$$

$$\rho_s \frac{d\delta}{dt} = \dot{m} \tag{11}$$

Combining (8), (9), (10), (11), and using the initial condition of $\rho_s = 0$ at $t=0$ for $z>0$,

$$C_1 t \frac{d\delta}{dt} - \sigma C_1 \delta = \sigma C_2, \tag{12}$$

which is a linear first order differential equation with the solution

$$\delta \exp\left(\int \frac{-\sigma}{t}\, dt\right) = \int \frac{\sigma C_2}{C_1 t} \exp\left(\int \frac{-\sigma}{t}\, dt\right) dt + C_4, \tag{13}$$

C_4 a constant. Integration of the above and use of the initial condition $\delta(0) = 0$ and final condition $\delta(t_f) = \delta_f$, the interface position at some time t may be expressed as

$$\delta = \delta_f \left(\frac{t}{t_f}\right)^{\sigma}. \tag{14}$$

Results for δ as a function of time for various values of the condensation coefficient are given in Figure 15. The time span of 7 hours is an estimate based on observation. The low value of $\sigma = .015$ is based on an experimentally obtained value of $\sigma = 0.0144 \pm 0.0020$ for solid ice between -13°C and -2°C (Delaney, Houston, and Eagleton, 1963), as opposed to values near unity reported by other authors (see Hobbs, 1974).

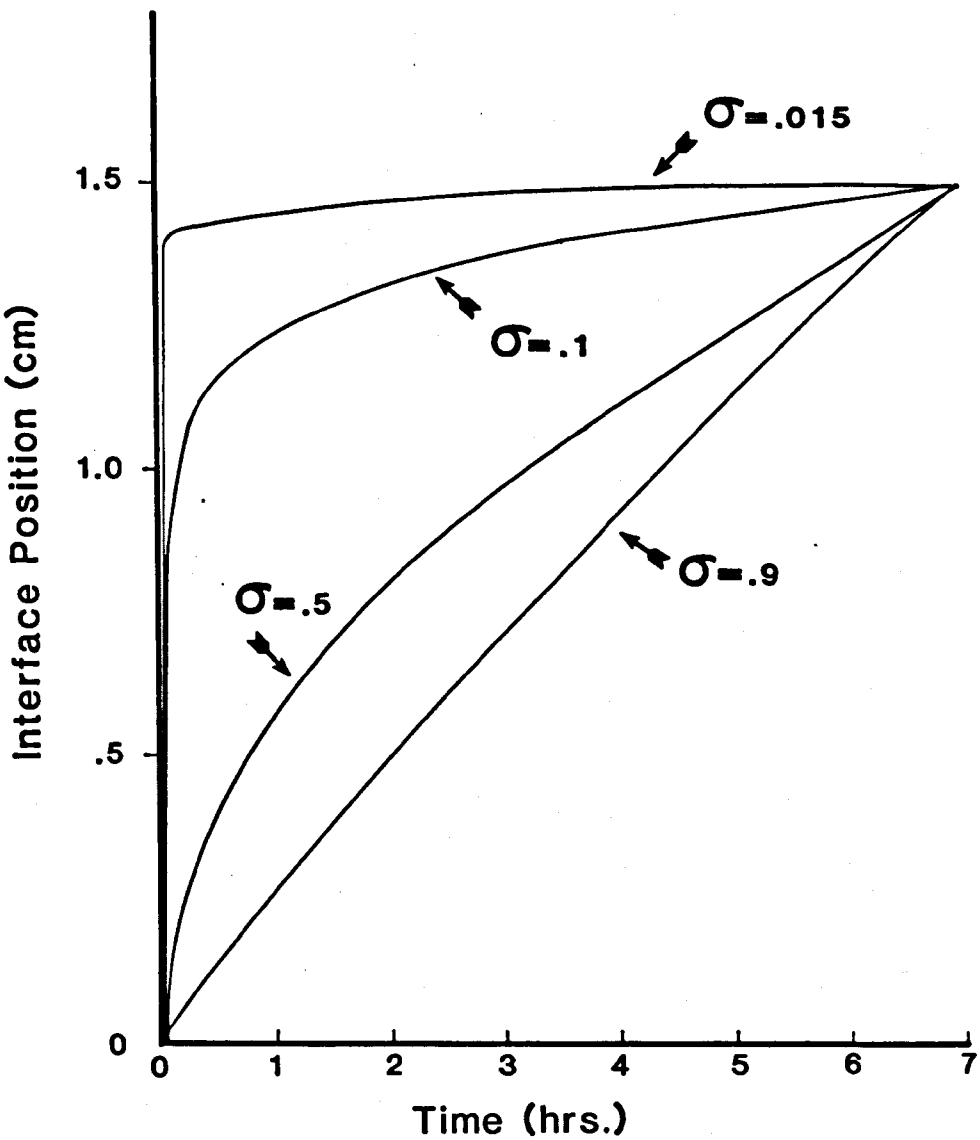

Figure 15. $\delta(t)$ vs. t.

Differentiation of (14) and combining with (11) gives an expression for the dispersed ice density as follows;

$$\rho_s = \frac{\dot{m}\, t_f^{\sigma}\, t^{1-\sigma}}{\sigma \delta_f} \tag{15}$$

which implies by use of (9) that $\dot{m}/t^{\sigma}$ is constant.

In order to obtain an estimate on the diffusive flux of vapour, consideration must first be given to a momentum equation for the binary gas mixture above δ. It is assumed that the stress in the fluid obeys the Navier-Poisson law for a fluid with no bulk viscosity. Furthermore, assuming that the only body force is gravity and neglecting local acceleration, a momentum equation may be written as

$$\frac{-dp}{dz} + 4/3\,\mu \frac{d^2\dot{z}}{dz^2} - \rho_g g = \rho_g \dot{z} \frac{d\dot{z}}{dz}, \tag{16}$$

where μ is the dynamic viscosity and $\dot{z}$ is the vertical component of the barycentric or convective velocity of the gas mixture (see for example, Malvern, 1969). Also

$$\rho_g = \rho_a + \rho_v \tag{17}$$

is the total gas density, and

$$p = p_a + p_v \tag{18}$$

is the total gas pressure. It is also allowable to express the total gas pressure p as a sum of the static and dynamic contributions, such that

$$p = p_d + p_{st}\,. \tag{19}$$

Then

$$\frac{dp}{dz} = \frac{dp_d}{dz} + \frac{dp_{st}}{dz}, \tag{20}$$

or

$$\frac{dp}{dz} = \frac{dp_d}{dz} - \rho_g g\,. \tag{21}$$

Substitution of (21) into (16) gives

$$\frac{-dp_d}{dz} = \rho_g \dot{z} \frac{d\dot{z}}{dz} - 4/3\,\mu \frac{d^2\dot{z}}{dz^2} \tag{22}$$

which gives the dynamic pressure gradient in terms of the inertial and viscous forces. However, a dimensional analysis of (22) readily shows that the dynamic pressure gradient is at least five orders of magnitude less than the static pressure gradient. Therefore the total pressure gradient may be approximated as the hydrostatic equation,

$$\frac{dp}{dz} \doteq -\rho_g g \tag{23}$$

A diffusive mass flux per unit time and area for the vapour, j_v, is defined by

$$j_v = \rho_v(\dot{z}_v - \dot{z}) \tag{24}$$

$$= \rho_v u_v \tag{25}$$

where again $\dot{z}$ is the mixture velocity. Therefore u_v is defined as the diffusion velocity of the vapour. Since

$$\dot{z} = \frac{1}{\rho_g}(\rho_v \dot{z}_v + \rho_a \dot{z}_a) \tag{26}$$

obviously

$$j_v + j_a = 0\,. \tag{27}$$

The diffusive mass flux results from "mechanical and thermal driving forces" (Bird, Stewart, and Lightfoot, 1960; de Groot and Mazur, 1962), and may include terms from ordinary (concentration) diffusion, pressure diffusion, forced diffusion and/or thermal diffusion. In this analysis, the primary "driving forces" are related to the concentration and temperature gradients. By assuming a linear relationship of the diffusive flux to the "driving forces," an expression for the diffusive mass flux of vapour may be written as

$$j_v = -\rho_g D_{va} \frac{dc_v}{dz} - \rho_g \frac{D_v^{\theta}}{\Theta} \frac{d\Theta}{dz}\,, \tag{28}$$

where c_v is the concentration of vapour, i.e.,

$$c_v = \frac{\rho_v}{\rho_g}, \tag{29}$$

Θ is the absolute temperature, D_{va} is the binary diffusion coefficient, and D_v^{θ} is the thermal diffusion coefficient (Grew and Ibbs, 1952). The Onsager reciprocity relations give

$$D_{av} = D_{va} \tag{30}$$

$$D_v^{\theta} = -D_a^{\theta} \tag{31}$$

(de Groot and Mazur, 1962; Jost, 1960). The expression for j_v may be rewritten by defining the thermal diffusion factor for the vapour as

$$\kappa_v = \frac{D_v^{\theta}}{D_{va}\, c_v\, c_a} \tag{32}$$

(Bird, Stewart, and Lightfoot, 1960), where

$$c_a = 1 - c_v \ . \tag{33}$$

Substitution of (32) and (33) into (28) gives

$$j_v = -\rho_g D_{va} \left[\frac{dc_v}{dz} + \frac{\kappa_v\, c_v\, (1 - c_v)}{\Theta} \frac{d\Theta}{dz} \right] . \tag{34}$$

At such low temperatures and pressures, it is allowable to approximate the behaviour of both the air/vapour mixture and the vapour itself as ideal, i.e.,

$$p = \rho_g R \Theta \tag{35}$$

and

$$p_v = \rho_v\, R_v\, \Theta \tag{36}$$

where R and R_v are the gas constants for the mixture and vapour respectively. Then (29) becomes

$$c_v = \frac{p_v\, R}{p\, R_v} \ . \tag{37}$$

Differentiation of the above gives

$$\frac{dc_v}{dz} = \frac{R}{R_v}\left(\frac{1}{p}\frac{dp_v}{dz} - \frac{p_v}{p^2}\frac{dp}{dz}\right) . \qquad (38)$$

Use of (17) and (18), and substituting (23), (35) and (36) into the above gives

$$\frac{dc_v}{dz} = \frac{R}{R_v}\left(\frac{\rho_v R_v \Theta \rho g}{(\rho R\Theta)^2} - \frac{\rho_v g}{\rho R\Theta}\right) . \qquad (39)$$

Collecting terms, and again using (29), an expression for the concentration gradient of vapour may be written as

$$\frac{dc_v}{dz} = \frac{c_v g}{\Theta}\left(\frac{1}{R} - \frac{1}{R_v}\right) . \qquad (40)$$

At such low temperatures

$$1 - c_v \doteq 1 . \qquad (41)$$

Substitution of (40) and (41) into (34), and dividing both sides by ρ_v gives an approximate expression for the diffusion velocity of the vapour;

$$u_v \doteq -D_{va}\left[\frac{g}{\Theta}\left(\frac{1}{R} - \frac{1}{R_v}\right) + \frac{\kappa_v}{\Theta}\frac{d\Theta}{dz}\right] . \qquad (42)$$

It is allowable to then separate the effects due to concentration and thermal diffusion by letting the contribution to u_v by ordinary diffusion be

$$u_{vc} = \frac{-D_{va}\, g}{\Theta}\left(\frac{1}{R} - \frac{1}{R_v}\right) \qquad (43)$$

and by thermal diffusion be

$$u_{v\theta} = \frac{-D_{va}\,\kappa_v}{\Theta}\frac{d\Theta}{dz} \qquad (44)$$

such that

$$u_v = u_{vc} + u_{v\theta} . \qquad (45)$$

Using the curve-fit temperature profiles in Figures 10 and 13, results for u_{vc} and $u_{v\theta}$ with respect to position are shown in Figures 19 and 20.

Two separate results are quite obvious. First, thermal diffusion is quite dominant, such that

$$u_v \doteq u_{v\theta} . \tag{46}$$

Regardless, the diffusive mass flux is totally insufficient to produce any significant amount of condensate, even with incredulous supersaturations. Therefore, convection must be the dominant mechanism for vapour transport. It then follows that the vapour velocity may be approximated as the convective velocity, i.e.,

$$\dot{z}_v \doteq \dot{z} . \tag{47}$$

Then by (24), (34) and (47), the concentration gradient of vapour is related to the temperature distribution as follows;

$$\frac{-1}{c_v} \frac{dc_v}{dz} = \kappa_v \frac{1}{\Theta} \frac{d\Theta}{dz} \tag{48}$$

Neglecting the temperature dependence of κ_v, integration of the above gives

$$c_v = C_6 \Theta^{-\kappa_v} , \tag{49}$$

where C_6 is a constant, and must be evaluated by assuming some condition of supersaturation. Substitution of (10), (29), (47), and (49) into (15) gives an approximate expression for the dispersed ice density as

$$\rho_s(t) \doteq \frac{-\rho_g(\delta)\, C_6\, [\Theta(\delta)]^{-\kappa_v}\, t_f^{\sigma}\, t^{1-\sigma}\, \dot{z}(\delta)}{\delta_f} . \tag{50}$$

This expresses the dispersed ice density at some time t as a function of the gas density, temperature and the vertical component of the convective velocity at the interface, degree of supersaturation and values of the thermal diffusion factor and condensation coefficient.

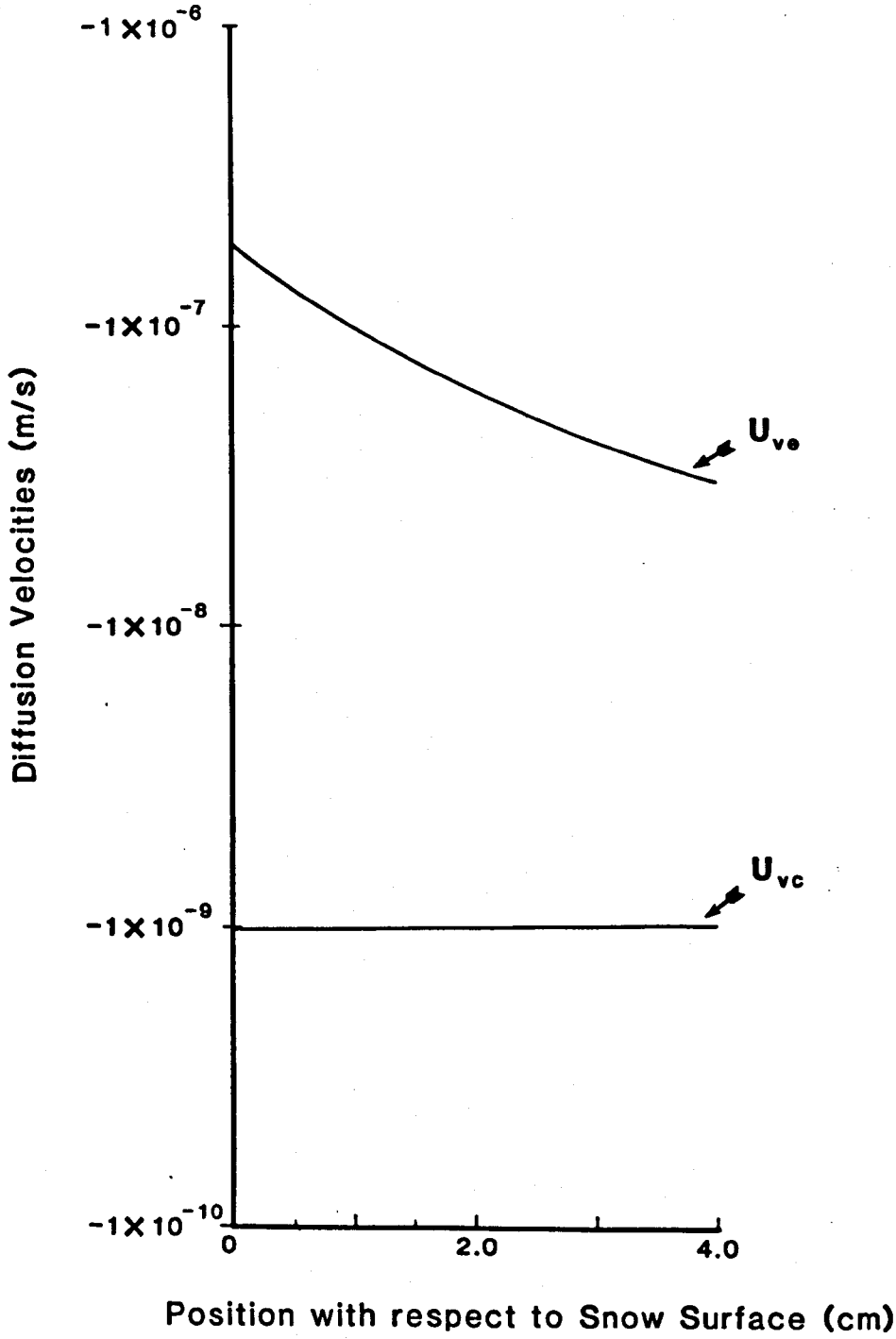

Figure 19. Calculated near-surface thermal and concentration diffusion velocities for 29-30 January.

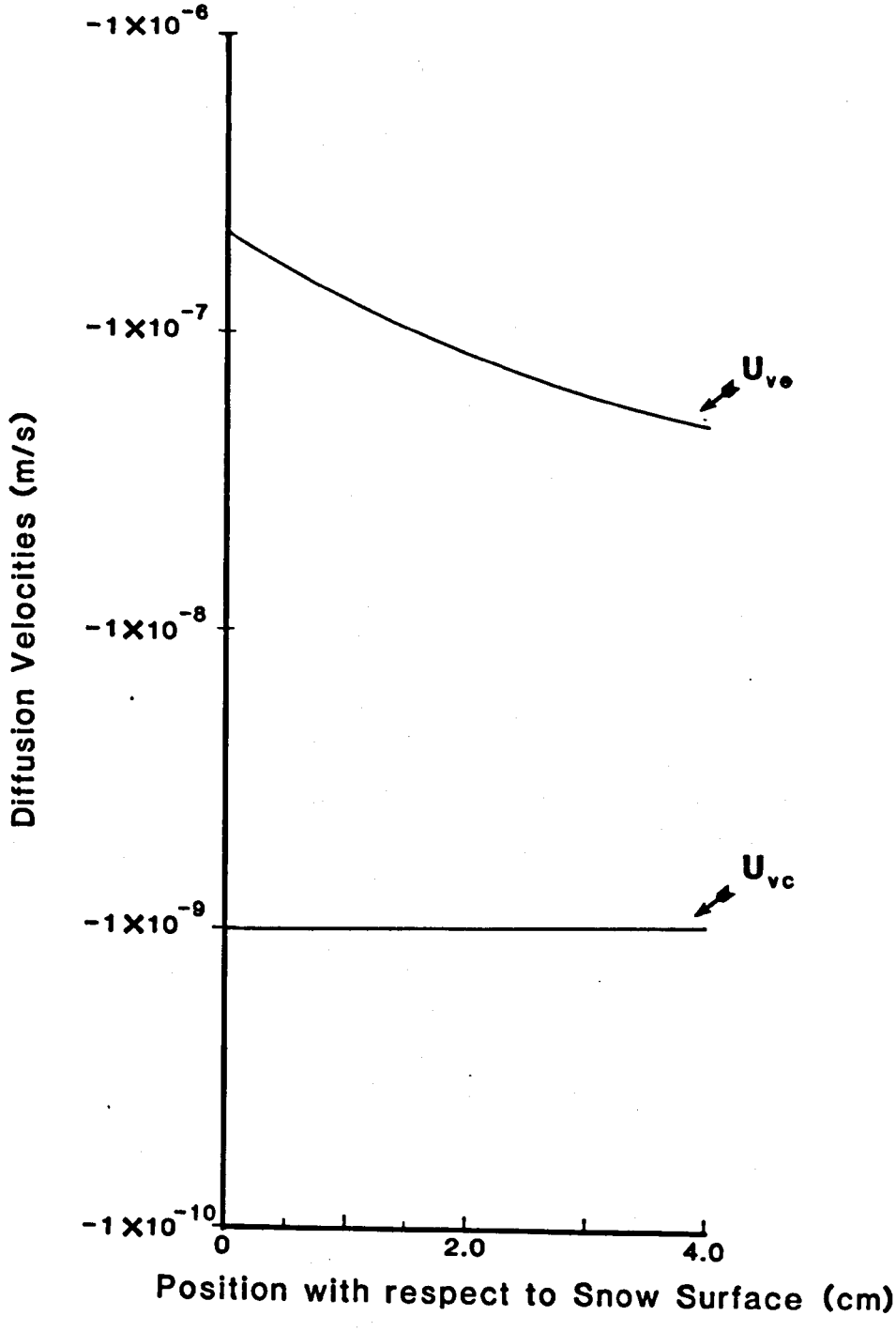

Figure 20. Calculated near-surface thermal and concentration diffusion velocities, 27-28 February.

An order of magnitude estimate on $\dot{z}$, gives $\dot{z} \doteq -1 \times 10^{-2}$ m/s to support a sufficient amount of condensate for surface hoar growth.

CHAPTER FIVE

RESULTS AND CONCLUSIONS

Observations in the condensation studies agreed very well with transition temperatures reported by Kobayashi (1961), which induce changes in preferential growth along the a-axes to c-axis growth, or vice versa. When the snow surface cooled to temperatures measured to be less than -21°C the end result was needle-like growth on the snow surface. During plate-like growth, measured snow surface temperatures ranged approximately between -12.5°C and -21°C. On numerous occasions, plates would begin to form on the snow surface, but as the snow surface temperature would continue to decrease, needle-type growth would predominate.

In either case, the crystals would retain the orientation of their initial nucleation site; an axis of an existing surface crystal. Sector plates or needles were usually oriented within a few degrees of surface normal, along the temperature gradient. Crystals exhibiting secondary growth features, such as dendritic hoar or rimed needles were more randomly oriented with respect to the snow surface, but within 60° of surface normal.

It was, indeed, surprising that the net accumulation of ice crystals on a variety of surfaces was macroscopically equivalent. So although initially some vapour is probably transported through the underlying snow to the snow surface, it seems to have a negligible effect on the net amount of condensate.

Furthermore, a large near-surface temperature gradient, due to nocturnal clear sky conditions, is insufficient in itself for significant condensation onto the snow surface to occur. Any detectable level of horizontal air motion near the surface was observed to prohibit growth. However, the total estimated diffusive flux of vapour is physically insufficient

for the amount of condensate, even assuming very high supersaturations. Realistically, the total vapour flux must be orders of magnitude larger than the resulting diffusive flux, which suggests that the actual vapour transport process is dominated by convection resulting from local temperature inequalities. The process of hoarfrost formation may therefore be a quasi-turbulent phenomenon. If the air is calm, the loss of vapour to the condensate could not be replenished rapidly enough by diffusion alone and condensation would cease. On the other hand, if air motion was too vigorous, the radiative cooling of the snow surface would be offset by turbulent warming and the vapour inversion would be destroyed. Furthermore, hoar growth would be prohibitive due to the fragility of the crystal itself.

Cloud cover conditions during the day must also be taken into consideration. If overcast skies prevail during the day, then subsequent clearing of the cloud cover at night causes the snow surface to cool rapidly to the frostpoint. Such conditions normally occur after the passage of a cold front, during which time the air adjacent to the snow surface acquires a high humidity due to heavy cloud cover and/or recent snow accumulation associated with the front. After the frontal passage, air pressure rises, skies clear, and temperature drops. (However, this sequence of events need not be endemic to more humid regions, or prerequisite during spring conditions, when surface hoar may develop at temperatures near 0° C.)

It is also noteworthy to report that although the net loss of heat from various ground surfaces during a high cirrus-type cloud cover is reported to be as great as when the sky is clear (Henson and Longley, 1944), the presence of high cirruform did interfere with longwave radiational cooling of the snow surface, and hence vapour flux to the surface. Similarly, it was observed that even during rapid growth rates, hoar would not form within small concavities on the snow surface, which implies that back radiation from within an incurvature is sufficient to prevent adequate surface cooling.

Another point of interest was that when the condensate was in the form of needles, shortly after sunrise they would be rapidly sublimated in areas exposed to insolation. But plate-type crystals were nearly unaffected by insolation, as discussed in Study 3. It has been suggested that the growth rate (and hence the sublimation rate) of kinetic growth forms is governed by the surface kinetics, which is reflected in variations of the condensation coefficient with respect to temperature and the c- and a-planes of ice (Lamb & Hobbs, 1971). Some exact information on the variation of condensation and sublimation coefficients with axial orientation and temperature could partially serve to explain the instability of needles vs. the stability of plates during insolation.

Once a surface hoar layer is incorporated into the snowpack, the assumption that the resulting instability rapidly subsides is extremely dangerous. Hoar layers may remain indefinitely in progressively more deteriorated forms, obscured by the presence of rounded grains which have either "sifted down" into the pore spaces or perhaps formed from the mass lost from the perimeters of the hoar crystals themselves. Of course, the smaller the hoar crystals, the more rapidly they are obscured. In some cases, hoar layers may be nearly unnoticeable, even at the snow surface immediately after their formation. Unfortunately, the initial basal shear strength of all surface hoar, whether a small sector plate or a large dendrite, is nearly non-existent.

One critical missing piece of information is the temperature profile through the hoar layer after its incorporation into the snowpack. During the winter months, a net negative temperature gradient is established in the snowpack. The high degree of porosity within a surface hoar layer combined with a negative temperature gradient should precipitate the development of similar kinetic growth form, depth hoar, at the expense of the surface hoar. Yet this was not observed to occur. Furthermore, observations indicate that marked deterioration of a surface hoar layer is effected only when the snowpack becomes isothermal at temperatures near 0° C.

In summary, it is sufficient to say that more information on the various properties of snow and ice is needed. Mass transfer processes at the snow surface and within the snowpack are not easily explainable and demand further attention. Steady one-dimensional flow is, at most, a poor description of the problem at hand.

LITERATURE CITED

LITERATURE CITED

Bird, R. B., Stewart, W. E., and Lightfoot, E. N. (1960). Transport Phenomena. Wiley, New York.

Brown, R. L., and Oakberg, R. G. (1982). Personal communications.

Caceci, M. S., and Cacheris, W. P. (1984). Fitting Curves to Data. Byte Magazine 9(5), 340-362.

Colbeck, S. C. (1982). Growth of Faceted Crystals in a Snow Cover, CRREL Report 82-29.

de Groot, S. R., and Mazur, P. (1962). Non-Equilibrium Thermodynamics. North Holland Pub. Co., Amsterdam.

Delaney, L. J., Houston, R. W., and Eagleton, L. C. (1964). The Rate of Vaporization of Water and Ice. Chem. Engng. Sci. 19, 105-114.

Fletcher, N. H. (1968). Surface Structure of Water and Ice. II. A Revised Model. Phil. Mag. 18, 1287-1300.

Fletcher, N. H. (1970). The Chemical Physics of Ice. Cambridge Univ. Press.

Grew, K. E., and Ibbs, T. L. (1952). Thermal Diffusion in Gases. Cambridge Univ. Press.

Haefeli, R. (1939). Snow Mechanics with References to Soil Mechanics, Bader et al., Der Schee und seine Metamorphose, Beiträge zur Geologie der Schweiz, Geotechnische Serie, Hydrologie, Liefurung 3, Bern. (U.S.A. SIPRE Translation No. 14, 1954.)

Hallett, J., and Mason, B. J. (1958). The Influence of Temperature and Supersaturation on the Habit of Ice Crystals Grown from the Vapour. Proc. R. Soc., A247, 440-453.

Henson, E. W., and Longley, R. W. (1944). Meteorology Theoretical and Applied. Wiley, New York.

Hobbs, P. V. (1974). Ice Physics. Clarendon Press, Oxford.

Jost, W. (1960). Diffusion in Solids, Liquids, Gases. Academic Press, New York.

Keeler, C. M., and Weeks, W. F. (1967). Some Mechanical Properties of Alpine Snow, Montana 1964-66. CRREL Report 227.

Keenan, J. H., Keyes, F. G., Hill, P. G., and Moore, J. G. (1978). Steam Tables. Wiley, New York.

Kobayashi, T. (1957). Experimental Researches on the Snow Crystal Habit and Growth by Means of a Diffusion Cloud Chamber. J. Met. Soc. Japan, 75, 38-44.

Kobayashi, T. (1961). The Growth of Snow Crystals at Low Supersaturation. Phil. Mag. 6, 1363-1370.

LaChapelle, E. R. (1969). Field Guide to Snow Crystals. Univ. of Washington Press.

Lamb, D., and Hobbs, P. V. (1971). Growth Rates and Habits of Ice Crystals Grown from the Vapour Phase. J. Atmos. Sci., 28, 1506-1509.

Luikov, A. V., and Mikhailov, Yu. A. (1965). Theory of Energy and Mass Transfer. Oxford, Pergamon Press, New York.

Malvern, L. E. (1969). Introduction to the Mechanics of a Continuous Medium. Prentice-Hall, Inc., New Jersey.

Martinelli, M., Jr. (1971). Physical Properties of Alpine Snow as Related to Weather and Avalanche Conditions. U.S.D.A. RM-64.

Mason, B. J., Bryant, G. W., and Van den Heuval, A. P. (1963). The Growth Habits and Surface Structure of Ice Crystals. Phil. Mag. 8, 505-526.

Mason, E. A., and Monchick, L. (1963). Survey of the Equation of State and Transport Properties of Moist Gases. Int. Symp. on Humidity and Moisture, N.B.S., Washington, D.C.

Nakaya, U. (1954). Snow Crystals. Harvard Univ. Press, Cambridge, Mass.

Nedler, J. A., and Mead, R. (1965). A Simplex Method for Function Minimization. Comp. J. 7, 308.

Oke, T. R. (1978). Boundary Layer Climates. Methuen and Co. Ltd., London.

Perla, R. (1977). Slab Avalanche Measurements. Can. Geotech. J. 14(2), 206-213.

Perla, R., Beck, T. M. H., and Cheng, T. T. (1982). The Shear Strength Index of Alpine Snow. Cold Reg. Sci. and Tech. 6, 11-20.

Roch, A. (1966). Les variations de la résistance de la neige. Int. Sym. on Sci. Aspects of Snow and Ice Avalanches, Int. Assn. of Hyd. Sci. 69, 86-99.

Shaw, D., and Mason, B. J. (1955). The growth of ice crystals from the vapour. Phil. Mag. 46, 249-262.

Sutton, O. G. (1953). Micrometeorology. McGraw-Hill, New York.

Voitkovsky, K. F. (1977). Mekhanicheskie svoystva snega. (Mechanical Properties of Snow). Nauka, Moscow.

MONTANA STATE UNIVERSITY LIBRARIES
arch N378.L255 RL
Studies on surface hoar : formation and
3 1762 00189985 3